Chapter 10
Operation and Control of Off-Grid Systems

10.1 Introduction

The previous chapters have given us the knowledge to understand how a mini-grid operates as a complete system, which we focus on in this chapter. We are primarily concerned with understanding how power flows through a mini-grid and, in particular, how the action of different controllers together affects the operation. The electrical aspects of the mini-grid take center stage, as we are less concerned with the physical details of the underlying energy conversion and storage technologies. This chapter begins by describing how a mini-grid manages the power to and from its batteries. We next develop a model of the mini-grid, which is useful in determining the flow of power under various conditions. Parallel operation of AC-coupled generators are then covered. The chapter concludes by presenting the algorithms used by maximum power point trackers to improve power production from PV arrays.

10.2 Battery Charging and Discharging

Off-grid systems that incorporate battery storage have special control requirements. The control scheme determines when to charge and discharge the battery and how this can be done in a way that prolongs the lifespan of the battery. This should be done without sacrificing the desired level of reliability and availability.

Some battery charging control schemes are simple. A series- or shunt-type controller can be used as described in the previous chapter. However, in many cases it is more complex, especially as the power output of the system exceeds several kilowatts. Often there is not a single controller that manages the charging and discharging of the battery. Rather, it is a coordinated effort among many charge and diversion load controllers. Charging and discharging also become complex in

the sense that sophisticated algorithms are used. Remember, the battery bank is a significant capital expense and is often the first major component to fail. Although lithium–ion (LI) batteries are increasing in popularity, especially in solar lanterns and solar home systems, lead–acid batteries are much more common in mini-grids. We therefore focus on lead–acid batteries and make comments regarding lithium–ion batteries when appropriate. The reader may wish to review Chap. 8 before continuing as many of the concepts introduced in that chapter will be used.

10.2.1   Charge Control

Lead–acid batteries must be carefully charged. In particular, they should be charged to avoid evolution of hydrogen and oxygen gas caused by overvoltage conditions and thermal-related degradation caused by excessive current. In addition to the basic function of restoring charge, proper battery charging can break up the sulfate crystals that reduce capacity and can replenish energy lost by self-discharge.

Chapter 9 introduced several circuits that can be used to charge a battery. The control strategy for shunt- and series-type charge controllers is similar. When the battery terminal voltage reaches a predefined threshold, the switch operates—closing in a shunt controller and opening in a series controller. This stops the battery from being charged. When the voltage drops below a predefined threshold, the state of the switch is reversed.

Higher-quality charge controllers use PWM to regulate the current into the battery as shown in Fig. 10.1. The charge controller uses sensors to measure the battery's terminal voltage. The measured voltage is used in a closed-loop control system that automatically adjusts the charging current to prevent the battery from being overcharged. The charging process consists of three-stages [5]:

1. Bulk stage
2. Absorption stage
3. Float stage

The time required to complete the three-stage process depends primarily on the battery's state-of-charge (SoC) when charging begins. Five to 10 h is a reasonable range. On occasion, a fourth "equalizing" stage is used for periodic maintenance. When charging LI batteries, only the bulk and absorption stages are used, and the charging is usually faster. The bulk, absorption, and float stages are identifiable from the plot of the battery terminal voltage, as shown in Fig. 10.2.

Figure 10.3 shows a schematic representation of a charge controller connected to a battery at the DC bus. For now, we will consider a simplistic case in that nothing else is connected to DC bus so that

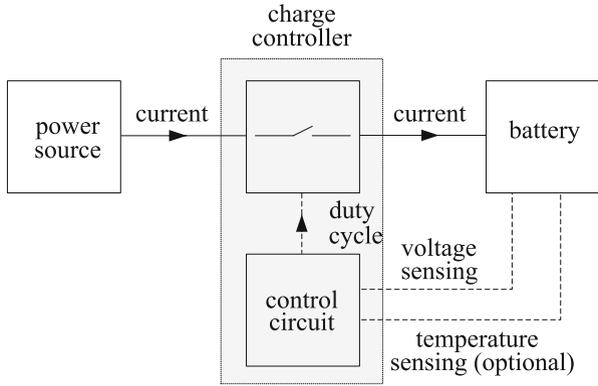$$I_{\text{CC}} = -I_{\text{B}}, \tag{10.1}$$

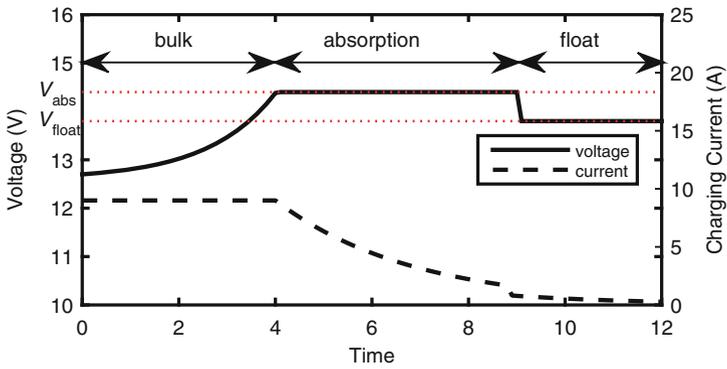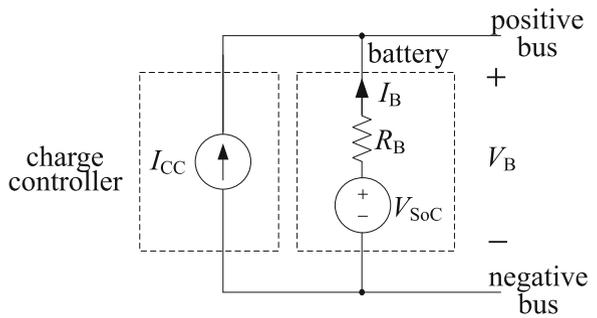**Fig. 10.1** Block diagram of a charge controller

Fig. 10.2 Idealized voltage and current profile of a 12 V lead–acid battery undergoing a three-stage charging process

Fig. 10.3 Circuit model of a charge controller and battery

and we note that the charge controller current I_{CC} is positive when charging the battery, whereas the battery current has the opposite polarity. Recall from Sect. 8.5.2 that the relationship between the terminal voltage V_B, the voltage representing the SoC V_{SoC}, current, and battery resistance R_B is

$$V_B = V_{SoC} - I_B R_B = V_{SoC} + I_{CC} R_B. \qquad (10.2)$$

We must always remember that the battery resistance depends on many factors, including the SoC and the magnitude of the battery current. We therefore interpret R_B as the battery resistance under the present conditions.

10.2.2   Bulk Stage of Charging

The bulk stage of charging begins when a battery is connected to the charger or when the input power to the charger is sufficient for it to operate. For example, a solar battery charger will begin the bulk charging stage sometime after sunrise.

The purpose of the bulk stage is to quickly charge the battery. Fast charging is desirable mostly for convenience. During the bulk stage, the battery's initial SoC is typically low, and so the battery is able to rapidly accept charge without worry of it being damaged by overvoltage. The current supplied by the controller is set to a predefined set-point value I_{CC}^*, which is typically no more than 13 to 20% of capacity at a C-rate of 0.05C. For example, I_{CC}^* should not exceed $0.20 \times 200 = 40$ A for a 200 Ah battery. The bulk stage is also referred to as the "constant current" stage. This is apparent from Fig. 10.2. Note that the controller is only able to supply its set-point current if there is sufficient power supplied to it. For now, we will assume this is the case. With nothing else connected to the DC bus, the terminal voltage is

$$V_B = V_{SoC} + I_{CC}^* R_B. \qquad (10.3)$$

Most of the charge provided to the battery regenerates the active material, with a small portion going toward unwanted side reactions. As the battery charge increases, V_{SoC} rises. The battery resistance increases as well. These effects together cause the terminal voltage to rise more rapidly, even though the charging current is constant. This is apparent from Fig. 10.2. The current remains constant until the battery terminal voltage reaches the absorption stage set-point voltage, V_{abs}. The bulk stage then ends and the absorption stage begins. The battery's SoC is typically between 70 and 80% when the bulk stage ends.

10.2.3   Absorption Stage of Charging

Continuing to charge at a high current risks damage to the battery. During the absorption stage, the charge controller automatically adjusts the battery current so that the terminal voltage remains constant at a predefined set-point V_{abs}. This is to avoid an overvoltage condition. The absorption stage is also known as the "constant voltage" stage. Figure 10.2 shows that unlike the bulk stage, it is the voltage that is constant and the current that is variable. The absorption set-point voltage is selected to be below the voltage at which gassing becomes problematic. For a nominal 12 V lead–acid battery, a set-point of 14.4 V (2.40 V/cell) is common. For a nominal 24 V battery, it doubles to 28.8 V and so on.

With $V_B = V_{abs}$, and with V_{SoC} and R_B continuing to rise as the battery charges, it is inevitable that I_{CC} decreases with time. The current from the charge controller is

$$I_{CC} = \frac{V_{abs} - V_{SoC}}{R_B}. \tag{10.4}$$

Because I_{CC} is decreasing, the rate at which the SoC increases slows. The current gradually decays as the difference between V_{SoC} and V_{abs} reduces, as shown in Fig. 10.2. The efficiency during the absorption stage is reduced as some gassing inevitably occurs at this higher voltage.

The absorption stage can be of fixed duration, for example, 4 h, or variable based upon an estimate of the most recent depth of discharge. Ideally, the absorption stage would end when the battery bank has reached a full SoC, but this cannot be precisely determined from the terminal voltage.

Example 10.1 A primary school is supplied with electricity by a stand-alone PV system. The PV module is used to charge a 12 V, 280 Ah lead–acid battery. At one point during the absorption stage, the battery resistance is 0.015 Ω/cell and V_{SoC} is 2.05 V/cell. Compute the current required to keep the terminal voltage at the absorption set-point of 14.4 V.

Solution A nominal 12V lead–acid battery has six cells in series. The terminal voltage of the battery is found from (10.4) to be:

$$I_{CC} = \frac{V_{abs} - V_{SoC}}{R_B} = \frac{14.4 - 6 \times 2.05}{6 \times 0.015} = 23.33 \text{ A}.$$

Example 10.2 Consider the same battery from the last example. Sometime later during the absorption stage, the battery resistance increases to 0.060 Ω/cell, and V_{SoC} increases to 2.10 V/cell. The absorption set-point is 14.4 V. Compute the current required to keep the terminal voltage at the absorption set-point of 14.4V.

Solution As before, the terminal voltage of the battery is found from (10.4) to be:

$$I_{\text{CC}} = \frac{V_{\text{abs}} - V_{\text{SoC}}}{R_{\text{B}}} = \frac{14.4 - 6 \times 2.10}{6 \times 0.060} = 5.0 \text{ A}.$$

We see that as the absorption stage progresses, the current decreases as V_{SoC} and R_{B} increase.

10.2.4 Float Stage of Charging

The float stage begins as the absorption stage ends. The two stages are similar in that the charge controller regulates the terminal voltage according to a predefined set-point. The float stage set-point V_{float} is lower than the absorption set-point V_{abs}, for example, 13.4 V (2.23 V/cell) for a nominal 12 V lead–acid battery. The purpose of this stage is to keep the battery fully charged by off-setting any self-discharge. The charge controller current is close to zero during the float stage, again assuming that there are no other components connected to the battery. The charge controller current required to regulate the terminal voltage at the float stage set-point is

$$I_{\text{CC}} = \frac{V_{\text{float}} - V_{\text{SoC}}}{R_{\text{B}}}. \tag{10.5}$$

Lithium–ion battery chargers do not include a float stage as the prolonged higher voltage shortens their lifespan.

10.2.5 Equalizing Stage of Charging

The equalizing stage is done periodically, perhaps once per month, to break up sulfate crystals that may have formed. The equalizing stage occurs immediately after the absorption stage. During this stage, the voltage is regulated at a much

higher voltage, for example, 15 to 16 V for a nominal 12V lead–acid battery. The battery current will be low, perhaps 3 to 6% of the battery's 20-h capacity rating. The stage lasts for 3 to 6 h. Some chargers automatically schedule equalizing; in others, the user must initiate it by pushing a button. The equalizing stage prolongs the total charging time. This can be a problem in PV-powered systems where the battery can only be charged during daylight hours. One solution is to reduce the overnight discharge the evening before the equalization is to take place. This allows the bulk and absorption stages to end early in the day, leaving sufficient time for the equalization stage to complete.

10.2.6   Power-Constrained Charging

The power provided by the charge controller is the product of the current it supplies and the DC bus voltage. Since the DC bus voltage is equal to the battery terminal voltage, we can write the charge controller output power $P_{CC,out}$ as

$$P_{CC,out} = V_B I_{CC}. \tag{10.6}$$

The power output from the charge controller is also equal to its input power $P_{CC,in}$ multiplied by the charge controller's efficiency:

$$P_{CC,out} = \eta_{CC} P_{CC,in} \tag{10.7}$$

where $P_{CC,in}$ is computed from the voltage and current at the input side of the charge controller. This can be, for example, a PV array or gen set.

When the power input to the charge controller is insufficient to maintain the bulk stage set-point current or the absorption or float stage voltage set-points, it is said to be "power-constrained." This often occurs in solar- and wind-powered mini-grids. A charge controller connected to a PV array might not be able to supply the bulk stage set-point current I_{CC}^* when it is cloudy, for example.

The maximum current I_{CC}^{max} that can be provided by the controller at a particular moment is the lesser of its set-point current and that allowed by its power supply

$$I_{CC}^{max} = \min \left\{ I_{CC}^*, \frac{\eta_{CC} P_{CC,in}^{max}}{V_B} \right\}. \tag{10.8}$$

where $P_{CC,in}^{max}$ is the maximum power that can be input to the charge controller by its source at a particular moment.
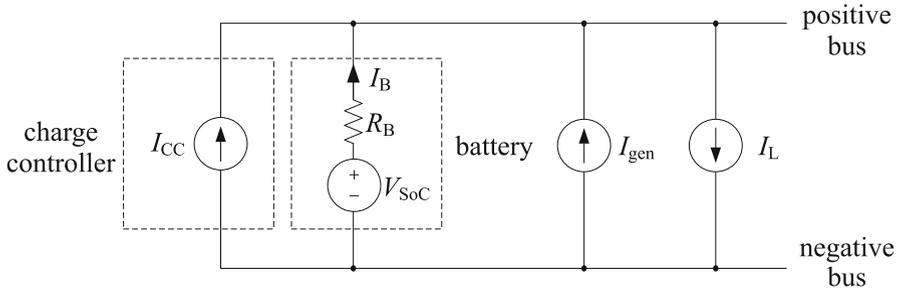
Fig. 10.4 Circuit model of DC bus with battery, charge controller, generator and load

10.2.7 Battery Charger Circuit Analysis

The previous section considered the simplest case of battery charging. In the absence of other generation sources, controllers, or load, the charge controller current is equal to the negative of the battery current. We now consider a more general case. Consider the mini-grid shown in Fig. 10.4. Here we have modeled the current from a generic generator and the load as constant current sources. The generator does not have its own controller, but it is connected to the DC bus through an uncontrolled rectifier, which is not explicitly modeled in the circuit diagram. This is sometimes the case when a WECS is used. The load can be connected to the DC bus directly or through an inverter. In either case, I_L is the load current as seen by the DC bus. Although only one generator and load are shown, the current I_{gen} and I_L can easily be replaced with the sum of the current from several generators and loads, respectively. We should not expect I_{gen} and I_L to ever be negative.

Applying Kirchhoff's Current Law at the positive DC bus:

$$I_B = -I_{CC} - I_{gen} + I_L. \tag{10.9}$$

From this we see that it is possible for the battery current to be positive, indicating that it is discharging, despite being connected to a charger.

The terminal voltage of the battery is

$$V_B = V_{SoC} - I_B R_B = V_{SoC} - \left(-I_{CC} - I_{gen} + I_L\right) R_B. \tag{10.10}$$

The current from the charge controller depends on the charging stage and whether or not the charge controller itself is power-constrained, as discussed next.

10.2.7.1 Bulk Stage

During the bulk stage, the current from the charge controller is equal to its maximum value I_{CC}^{max} (the lesser of the set-point current or power-constrained current). The corresponding battery current and terminal voltage can be computed from (10.9) and (10.10) by replacing I_{CC} with I_{CC}^{max}.

10.2.7.2 Absorption and Float Stages

In the absorption stage, the charge controller acts to balance the changes in net load and generator current to maintain the terminal voltage at V_{abs}. The *required* charge controller current $\hat{I}_{CC}$ to maintain the terminal voltage at the absorption set-point is

$$V_B = V_{abs} \tag{10.11}$$

$$\hat{I}_{CC} = \frac{V_{abs} - V_{SoC}}{R_B} + I_L - I_{gen}. \tag{10.12}$$

However, the actual charge controller current might not be $\hat{I}_{CC}$. The charge controller current cannot be negative; otherwise, it would be a load. The charge controller also cannot supply current above its maximum current as determined by (10.8). Therefore, the actual charge controller current is

$$I_{CC} = \begin{cases} 0 & : \hat{I}_{CC} \leq 0 \quad \text{(Overvoltage)} \\ \hat{I}_{CC} & : 0 < \hat{I}_{CC} < I_{CC}^{max} \\ I_{CC}^{max} & : \hat{I}_{CC} \geq I_{CC}^{max} \quad \text{(Undervoltage)} \end{cases} \tag{10.13}$$

Whenever $I_{CC} \neq \hat{I}_{CC}$, the absorption set-point voltage is not maintained and $V_B \neq V_{abs}$. Instead, the battery's terminal voltage is found using (10.10). The terminal voltage can be higher or lower than the absorption set-point. It is higher when there is excessive current from other generators; it is lower when the load current is too large. Neither condition is desirable. However, overvoltage is worse as it can damage the battery; undervoltage indicates that the battery is not being charged at the desired rate or is even being discharged.

If the load is constant, then an increase or decrease in I_{gen} is countered by an equal and opposite change in $\hat{I}_{CC}$ as seen in Fig. 10.5a. However, near the center of the plot, the generator current becomes so low that $\hat{I}_{CC} > I_{CC}^{max}$. The charge controller produces its maximum current, but this is insufficient to regulate the battery voltage at V_{abs}. This is seen by the dip in Fig. 10.5b. Similarly, when the generator current increases near the end of the plot, $\hat{I}_{CC}$ is negative, and so from (10.13) the actual charge controller current is zero. The battery voltage rises past the absorption set-point voltage. In practice, the charge controller will not be able to perfectly and instantly balance the changes in net load and generation even if $0 < \hat{I}_{CC} < I_{CC}^{max}$. Some slight fluctuation in the terminal voltage is therefore to be expected.

The analysis of the float stage is similar to the absorption stage, but V_{abs} is replaced with V_{float} in (10.12). As in the absorption stage, it is possible for the load current to be such that the float voltage cannot be maintained.

To prevent overvoltage, it is important that any source supplying current to the battery be connected to the DC bus through a charge controller (or a bi-directional converter with battery charging feature) or for there to be a diversion load, as discussed in the following section.
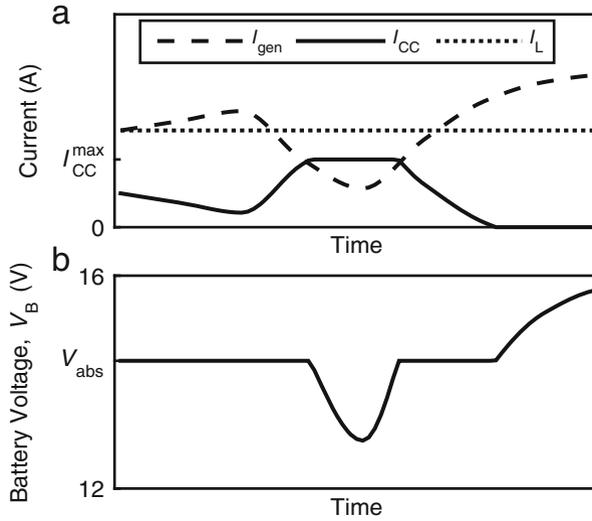
Fig. 10.5 (**a**) The charge controller current balances the change in generator current unless the charge controller's limits are reached (**b**) the battery voltage is constant when the charge controller is able to balance changes in the generator current

Example 10.3 Consider a hybrid DC-coupled mini-grid consisting of a PV array with charge controller, MHP generator with uncontrolled rectifier, and a battery. Let $V_{abs} = 14.4$ V, and $R_B = 0.075\ \Omega$. Compute the absorption stage charge controller current when $V_{SoC} = 12.5$ V. The load is 8 A. The current from the generator is 36 A. The charge controller is rated at 30 A, has an efficiency of 98%, and is supplied by a PV array whose input power is 300 W.

Solution We first calculate the charge controller current required to maintain the terminal voltage at 14.4 V using (10.12)

$$\hat{I}_{CC} = \frac{V_{abs} - V_{SoC}}{R_B} + I_L - I_{gen} = \frac{14.4 - 12.5}{0.075} + 8 - 36 = -2.67 \text{ A}.$$

Immediately we see that the charge controller cannot provide this current as it is negative. Applying (10.13), we set $I_{CC} = 0$ A. The charge controller is unable to maintain the absorption stage set-point. We can determine the battery voltage using (10.10) to be:

$$V_B = V_{SoC} - \left(-I_{CC} - I_{gen} + I_L+\right) R_B = 12.5 - (0 - 36 + 8)\,0.075 = 14.6 \text{ V}.$$

The battery is being overvoltaged by 0.2 V. To prevent this overvoltage, either the MHP generator current must be decreased or the load increased.
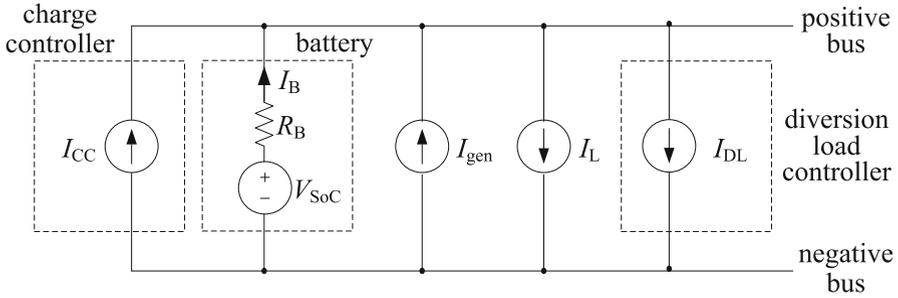
Fig. 10.6 Circuit model of a mini-grid with a diversion load

10.2.8 *Diversion Load Control*

Diversion loads are connected to the DC bus of the system through a diversion load controller. The diversion load controller is usually a PWM-controlled chopper circuit. It controls the current to the diversion load I_{DL}. The hardware and control circuitry of a diversion load controller is nearly identical to a charge controller. Instead of regulating the battery voltage by controlling current injected into the DC bus, the current withdrawn from the DC bus into the diversion load I_{DL} is controlled. In fact, diversion load controllers and charge controllers are so similar that some manufacturers produce a single unit that can function as either one (not simultaneously). The user selects the mode while configuring the set-points. The diversion load controller set-points for the absorption and float stages are designated $V_{abs,DL}$ and $V_{float,DL}$, respectively.

A mini-grid with diversion load is shown in Fig. 10.6. Applying Kirchhoff's Current Law at the positive bus:

$$I_B = -I_{CC} - I_{gen} + I_L + I_{DL}. \tag{10.14}$$

The terminal voltage of the battery is

$$V_B = V_{SoC} - I_B R_B = V_{SoC} - \left(-I_{CC} - I_{gen} + I_L + I_{DL}\right) R_B. \tag{10.15}$$

Similar to a charge controller, the diversion load controller current I_{DL} is limited between zero and its maximum value. The maximum value is based on the resistance of the diversion load R_{DL} and can be computed as

$$I_{DL}^{max} = \frac{V_B}{R_{DL}}. \tag{10.16}$$

Although the maximum current will vary somewhat based on the battery terminal voltage, we will make the assumption that it is a constant value. Like all resistors, diversion load resistors have a resistance value and a power rating. The power

rating is based on the power that the resistor can dissipate without overheating. The diversion load's power rating should be such that it can dissipate the total power from the DC bus generators that do not have a charge controller of their own. For example, a system with two 3 kW WECS and one 5 kW PV array (with its own charge controller) requires a diversion load rated at $2 \times 3 = 6$ kW. It is often prudent to somewhat oversize the diversion load in case of unexpected operating conditions.

The mini-grid modeled in Fig. 10.6 has two controllers: a charge controller and diversion load controller. The absorption and float voltage set-points must be carefully coordinated between the controllers. Current should never flow through the charge controller and diversion load controller at the same time. The additional current from the charge controller can cause the diversion load to overheat, potentially causing a fire. In theory, the set-points can be exactly the same, but in practice, even with identical set-points, small measurement error can lead to the diversion load overheating. Instead, the diversion load controller set-points are made slightly higher than the charge controller set-points

$$V_{\text{abs,DL}} = V_{\text{abs}} + \Delta \tag{10.17}$$

$$V_{\text{float,DL}} = V_{\text{float}} + \Delta \tag{10.18}$$

where Δ is perhaps 0.1 V.

### 10.2.8.1   Bulk Stage Charging with Diversion Load

If the absorption set-points are programmed according to (10.17), then the diversion load current during the bulk stage is $I_{\text{DL}} = 0$. As usual, $I_{\text{CC}} = I_{\text{CC}}^{\text{max}}$, and the terminal voltage is found using (10.15). From (10.17), the charge controller absorption set-point will be reached first, and the charge controller will enter the bulk stage before the diversion load controller does.

10.2.8.2   Absorption and Float Stage Charging with Diversion Load

During the absorption and float stages, the charge controller current is controlled as before. The diversion load will not draw current unless the battery voltage rises to the diversion load controller's absorption set-point $V_{\text{abs,DL}}$. If the charge and diversion load controllers are properly coordinated, then the battery voltage will only reach $V_{\text{abs,DL}}$ when $\hat{I}_{\text{CC}} < 0$. This occurs when the current from the generators is excessive. If the diversion load controller absorption voltage set-point is reached, then the diversion load current will increase to regulate the battery voltage at $V_{\text{abs,DL}}$. This is shown in Fig. 10.7. Compare this result to Fig. 10.5 where there is no diversion load.

The current required by the diversion load controller $\hat{I}_{\text{DL}}$ to regulate the battery voltage at $V_{\text{abs,DL}}$ is

Fig. 10.7 (**a**) The current from the diversion load increases near the end of the plot to regulate the voltage as the generator current increases. (**b**) The voltage is regulated at $V_{abs,DL}$ when current is supplied to the diversion load
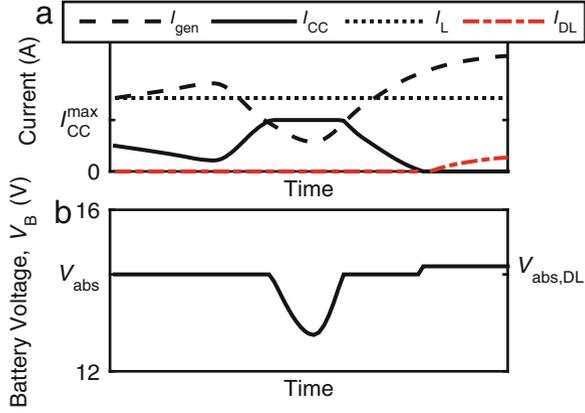
$$\hat{I}_{DL} = -\frac{V_{abs,DL} - V_{SoC}}{R_B} - I_L + I_{gen} + I_{CC}. \tag{10.19}$$

The actual diversion load current when $V_B > v_{abs}$ is

$$I_{DL} = \begin{cases} 0 & : \hat{I}_{DL} \leq 0 \quad \text{(Undervoltage)} \\ \hat{I}_{DL} & : 0 < \hat{I}_{DL} < I_{DL}^{max} \\ I_{DL}^{max} & : I_{DL}^{max} \leq \hat{I}_{DL} \quad \text{(Overvoltage)} \end{cases} \tag{10.20}$$

In a well-designed system, $\hat{I}_{DL}$ will never exceed I_{DL}^{max}. However, should it do so, the terminal voltage is found using (10.15). If the set-points of the controllers are set properly, then I_{DL} and I_{CC} will never simultaneously be positive. The diversion load current during the float stage is similarly computed using (10.19) and (10.20) but using the diversion load controller's float voltage set-point instead.

10.2.9   Coordinating Controller Set-Points

In systems with higher capacities, multiple charge controllers are often needed. See, for example, Fig. 10.8. A mini-grid might have several PV strings, each capable of producing high enough current or voltage that they require their own charge controller. In these systems, the controllers should be of the same model and have identical set-points. The charge controllers can then operate autonomously without communication to each other. As detailed previously, the set-points for diversion load controllers should be slightly higher than that of the charge controllers. If multiple diversion load controllers are needed, they all should have the same set-points.
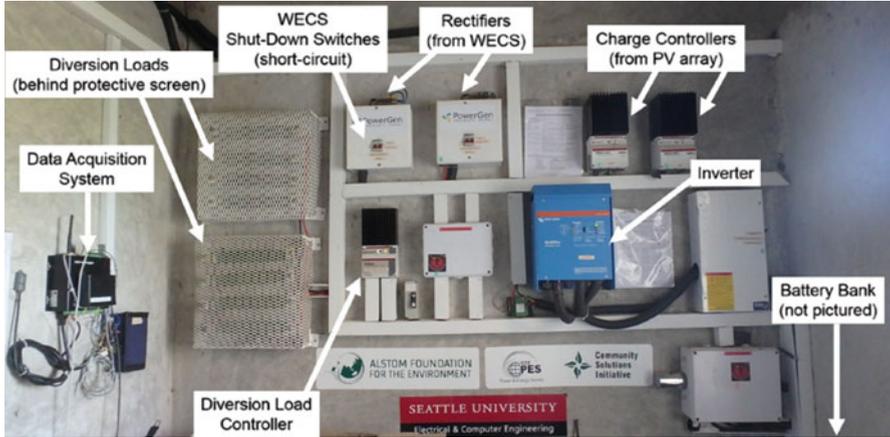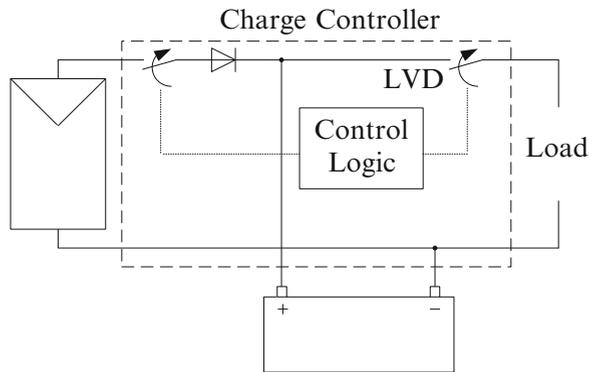
Fig. 10.8 The control room of a 5 kW hybrid wind/solar mini-grid in Kenya. Note the dual charge controllers and rectifiers (courtesy of author)

Fig. 10.9 LVD incorporated into a charge controller

10.3 Battery Discharge Control

Batteries should be prevented from excessive discharge to avoid permanent damage. This is usually achieved by disconnecting the load when the terminal voltage of a battery falls below a certain threshold. This feature is realized through a *low-voltage disconnect* (LVD). A solid-state switch with high current rating, typically a power MOSFET, is placed in series between the load and battery. A voltage sensor measures the battery terminal voltage. A signal is sent to the switch to disconnect the load if the measured value falls below a predefined disconnect set-point voltage $V_{\text{dis,LVD}}$. A LVD can be incorporated into a charge controller, as shown in Fig. 10.9, and/or the inverter and individual loads.

Care must be taken in determining the set-point value of V_{LVD}. The battery's internal voltage drop during discharge must be accounted for. A simple procedure

is to consult the battery's specification sheet to determine the steady-state open circuit voltage V_{SoC} corresponding to the SoC the LVD is desired to operate at. The anticipated internal voltage drop $I_B R_B$ is subtracted from V_{SoC} to determine the set-point of $V_{dis,LVD}$. Failure to correct for the internal voltage drop will result in the battery disconnecting prematurely. That the LVD does not directly measure the battery's SoC directly is an important and often misunderstood limitation of a LVD. It can be exploited to discharge the battery more deeply than expected, as explored further in the following example.

Example 10.4 A solar home system with a nominal 12 V AGM lead–acid battery powers two lights, each drawing 0.5 A. To prolong the life of the battery, the LVD should disconnect both lights when the battery reaches a SoC of 50%, corresponding to an open-circuit voltage of 12.24 V (see Table 8.1). Determine the LVD disconnect set-point if the battery resistance during discharge at a 50% SoC is 0.4 Ω. If the user only powers one light instead of two, will the LVD prevent the battery from being discharged to less than 50% SoC?

Solution The LVD disconnect set-point should be

$$V_{dis,LVD} = V_{SoC} - I_B R_B = 12.24 - 2 \times 0.5 \times 0.4 = 11.84 \text{ V}$$

If the user only uses one light, then the battery terminal voltage when 50% discharged is

$$V_B = V_{SoC} - I_B R_B = 12.24 - 1 \times 0.5 \times 0.4 = 12.04 \text{ V}$$

This is above the LVD voltage, and so power will continue to be supplied to the light, draining the battery further. The LVD will actuate when $V_B = V_{dis,LVD} = 11.84$ V. The SoC voltage will be:

$$V_{SoC} = V_B + I_B R_B = 11.84 + 1 \times 0.5 \times 0.4 = 12.04 \text{ V}$$

corresponding to a SoC of 25%, assuming R_B curve does not change. This is much lower than the target of 50% and will result in a shorter lifespan than the designer intended.

Solar home system users have been known to exploit the load dependence of the battery voltage drop to continue supplying some of the load past the designed minimum SoC target.

Fig. 10.10 Operation of low-voltage disconnect as a 24 V battery bank is discharged and recharged
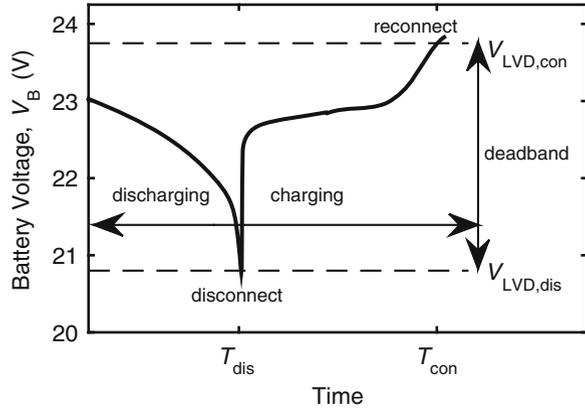
As soon as the LVD disconnects the load, the battery terminal voltage will quickly and sharply rise above $V_{\mathrm{LVD,dis}}$. This is shown in Fig. 10.10 at time T_{dis}. This occurs even if the battery is not immediately recharged, as the voltage drop internal to the battery $I_B R_B$ becomes zero. Additional voltage rise may occur due to mixing of the battery electrolyte.

The battery should be reconnected to the load after its SoC has increased. Reconnection occurs only after V_B exceeds a second set-point value $V_{\mathrm{LVD,con}}$ where $V_{\mathrm{LVD,con}} > V_{\mathrm{LVD,dis}}$. This occurs in Fig. 10.10 at time T_{con}. The difference between the reconnect and disconnect voltages is known as the "deadband." The reconnect voltage does not need to be the fully charged open-circuit voltage. However, it should be high enough to prevent nuisance disconnect—reconnect oscillations and attempts to defeat the LVD described in Example 10.4. For example, if the disconnect set-point is 11.5 V, then $V_{\mathrm{LVD,con}}$ could be set to 12.6 V.

High-quality LVD systems will use dedicated voltage sensor wires that carry very low current to reduce the voltage drop between the LVD circuit and the battery terminals. They will also compensate the set-points based on battery temperature—increasing the disconnect voltage as temperature rises. Other improvements are possible, for example, adjusting the LVD set-point based upon the measured discharge current, so that under higher discharge current, the set-point voltage is reduced.

Solar home systems and solar lanterns usually feature a LVD. Some are remotely configurable so that the LVD set-points can be adjusted based upon the user's behavior. In certain business models, this feature can be used to allow customers to "upgrade" their solar home system after purchase by paying to reduce the LVD set-point.

10.4   Charge and Diversion Load Controller Practical Considerations

Charge controllers are commercially available with a wide variety of features and ratings. They are typically rated based on their bulk-stage current, compatibility with battery nominal voltages, and input power or voltage and current ratings. Manufacturers often describe their solar charge controllers as "MPPT" or "PWM" (pulse width modulation). The former have integrated maximum power point trackers, as discussed in the previous chapter, whereas the PWM do not. This is somewhat confusing because most MMPT trackers also use pulse width modulation in controlling the built-in DC–DC converter. Higher-end charge controllers include a display of battery voltage and charging stage, and an integrated data acquisition and remote monitoring system. Some might include a SoC indicator, but these are often inaccurate and are best used as a general indicator rather than an exact measure.

Diversion load controllers are sometimes referred to as "wind turbine" charge controllers. The reason for this is that diversion loads are needed with WECS— WECS cannot be controlled by a series-regulated controller without risking an overspeed or overvoltage. However, a diversion load controller does not control the wind turbine—it controls the current to the diversion load.

It is very important to properly set and coordinate the absorption and float set-points of all controllers. Most charge controller manufacturers provide recommended settings based on the type of battery being charged; see, for example, Table 10.1. Battery manufacturers will usually provide values for the set-points, which should be followed.

Table 10.1 Typical charging set-points for a 24 V system

Battery	Absorption	Float	Equalization
AGM	28.2	27.6	31.8
Flooded lead–acid	28.8	27.6	32.4
LiFePO$_4$	28.4	27.0	–

In Chap. 8, we saw that the open-circuit voltage and battery resistance of lead–acid batteries are affected by temperature. At all but the lowest electrolyte concentration levels, the terminal voltage increases with temperature, whereas the battery resistance decreases with temperature. Gassing also occurs at a lower voltage as temperature increases. The set-points of the charge controller should be adjusted to account for these changes. Despite the increase in the voltage V_{SoC} with increasing temperature, the controller set-points should be *decreased* as temperature increases. For example, for a 24 V nominal lead–acid battery, the absorption and float stage voltage set-points are decreased by 0.032 V for every degree Celsius increase in temperature above the rated value. Higher-quality charge controllers with temperature sensors will automatically make this adjustment.

10.5   Interpreting Battery Voltage Profiles

A lot can be inferred from the daily or weekly profile of the battery bank voltage. In fact, the battery terminal voltage is perhaps the single most important and useful quantity to measure in an off-grid system. The interpretation of the profile is part art and part engineering. The profile provides insight into whether or not the controllers are functioning properly. It further provides information on whether the energy supply is appropriately sized to meet the load. It can also be used in troubleshooting technical problems. We will consider examples of daily operation from an actual 1.8 kW PV-powered mini-grid next. Each example considers a different day. In each example, three plots will be presented: the power from the PV array, the power to the inverter (load) and the battery bank's terminal voltage over a 24-h period.

To begin, consider the three plots in Fig. 10.11. The battery voltage profile is indicative of a healthy, properly functioning mini-grid. The three charging stages are distinct. The controller is able to rapidly charge the battery during the bulk stage. The controller tightly regulates the terminal voltage during the absorption and float stages, indicating that the controller is appropriately sized and not power-constrained. Notice how the power from the PV array begins to decay as soon as the absorption stage beings. This is not caused by a decrease in irradiance, but rather there is no need for additional power to be produced as the battery is nearly full and the load is low. The bulk charging is completed by 8:00, and the absorption stage is finished a few hours later. The charging is complete several hours before sunset; and we conclude the system can supply additional load during the evening and still be fully charged during the day.

In mini-grids powered by variable sources such as PV or WECS, the voltage profile will often not look like Fig. 10.11. Figure 10.12 is from the same mini-grid on a different date. The load is much higher than for the day depicted in Fig. 10.11. We see the battery voltage fluctuates during the absorption stage, indicating that the charge controller was power-constrained and unable to regulate the terminal voltage. This is most likely due to partial cloud coverage. The float stage is not reached before sunset. We should not be overly worried. The battery still spent considerable time in the absorption stage and is likely nearly full.

Now consider the voltage profile in Fig. 10.13. This is again for the same system as in Figs. 10.11 and 10.12. During this day, the absorption voltage is never reached, and so the charge controller never progresses past the bulk charging stage. As a result, the voltage lacks the distinct plateaus shown in the previous figures. This is a sign that during this day, the energy supplied by the battery is more than was input to it. This is obviously not sustainable in the long-term. Should the load not be reduced or the PV power increase, perhaps from increased irradiance or by cleaning the PV array, then the voltage will continue to decrease until the LVD actuates. This variability in supply is one reason that the reliability of gen sets are appealing.

To an untrained eye, it might appear that the battery is being properly charged. For example, for a 24 V nominal system, the open-circuit steady-state voltage is 25.2 V. The voltage profile in Fig. 10.13 exceeds this for most of the afternoon. This could lead to the erroneous conclusion that the battery is fully charged or even
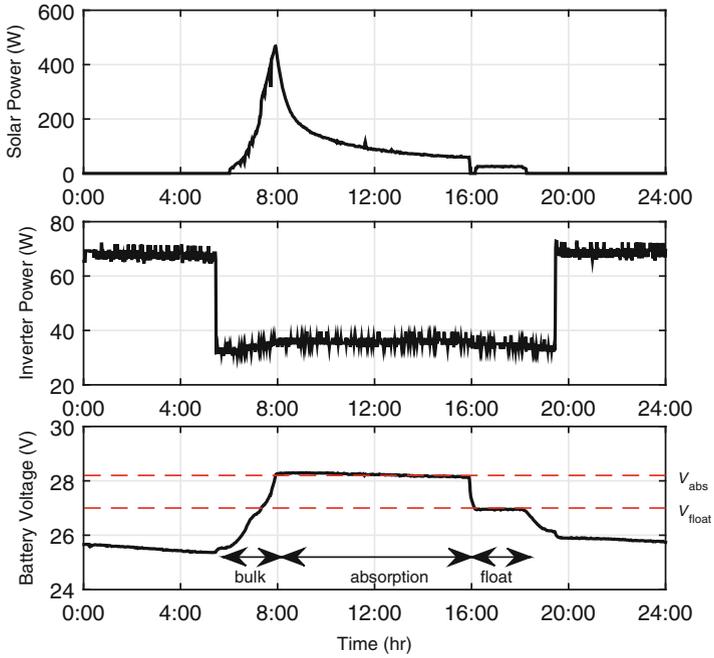
Fig. 10.11 The solar power, inverter power, and voltage profile of a mini-grid exhibiting typical behavior
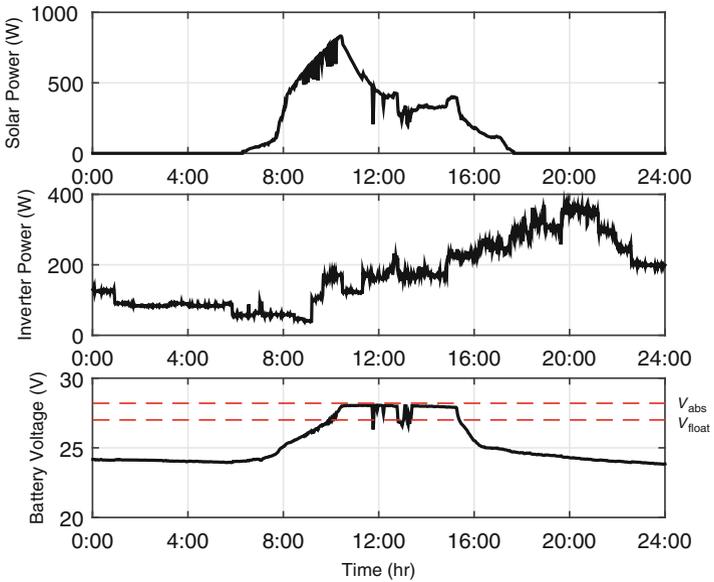

Fig. 10.12 The solar power, inverter power, and voltage profile of a mini-grid showing the operation of power-constrained charge controller during the absorption stage
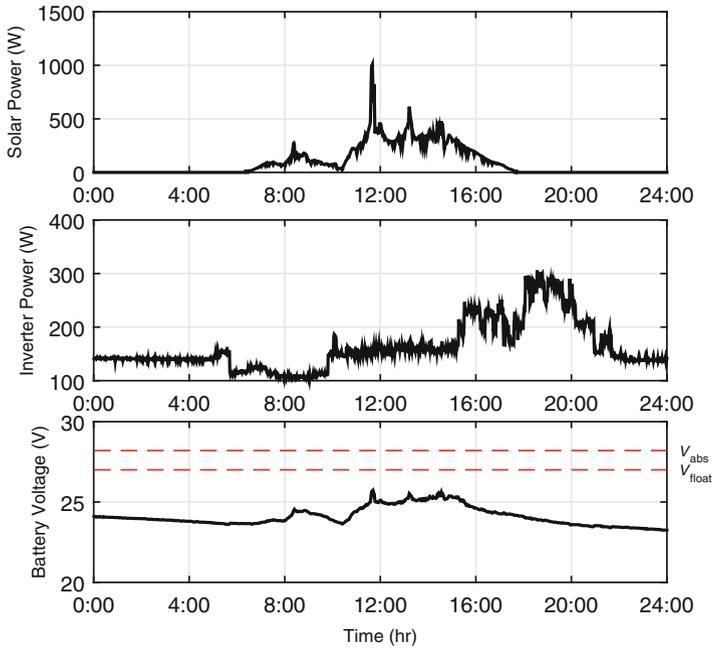
Fig. 10.13 The solar power, inverter power and voltage profile of a mini-grid showing the operation on a cloudy day

overcharged. It is easy to forget that the battery terminal voltage should not be used to infer the SoC unless the battery is open-circuit and has rested. Neither of those conditions apply to an active mini-grid.

10.6   Power Flow Model

We next develop a model that lets us calculate the flow of power from, to, and through the various components of a mini-grid. It is a steady-state algebraic model. Power flow models of this type are used in computer programs that simulate the operation of mini-grids. These simulation programs are described in Chap. 12. The model pertains to the energy production system of the mini-grid, not the distribution system. A more complicated nonlinear power flow model is needed to determine the flow of power in the distribution system [6].

The reader may recall from a course on basic circuit analysis that the sum of the real power produced by all the sources in a circuit equals the sum of the real power consumed by the loads. This is an extension of the more general law of conservation of energy and is the basis of the power flow model. When applied to a mini-grid with J components, the conservation of power is written as
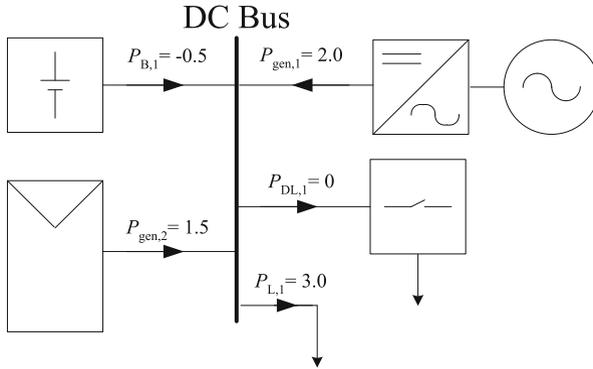
Fig. 10.14 Example of power flow in a mini-grid

$$\sum_{j=1}^{J} P_j = 0 \tag{10.21}$$

where P_j is the power associated with a component j, which could be a generator, load, or battery. This equation is the basis of the power flow model. Readers well-versed in circuit analysis should keep in mind that (10.21) and those that follow are in reference to the average real power, not the instantaneous power.

We adopt the convention that the power associated with a generator is positive when the generator is producing power and the power associated with a load is positive when it is consuming power. The power associated with these components will never be negative. Batteries follow the convention that the power is positive when discharging (supplying power) and negative when charging (consuming power).

Rewriting (10.21) using these conventions

$$\sum_{g=1}^{G} P_{\text{gen},g} + \sum_{b=1}^{B} P_{\text{B},b} - \sum_{l=1}^{L} P_{\text{L},l} - \sum_{m=1}^{M} P_{\text{DL},m} - \sum_{n=1}^{N} P_{\text{BL},n} = 0 \tag{10.22}$$

where $P_{\text{gen},g}$, $P_{\text{B},b}$, $P_{\text{L},l}$, $P_{\text{DL},m}$, and $P_{\text{BL},n}$ are the power associated with the G generators, B batteries, L loads, M diversion loads, and N ballast loads of the mini-grid, respectively. Recall from Chap. 9 that a ballast load acts like a diversion load but on the AC bus. Since we are focused on the electrical aspects of the system, the term "generator" refers to any energy conversion technology that generates electricity. This equation shows that the power associated with any component can be algebraically determined if the power of all other components is known. Figure 10.14 shows an example of the power flow in a DC-coupled mini-grid. The reader should verify that (10.21) is obeyed.

In general, we will consider the system batteries collectively as one battery bank so that

$$\sum_{b=1}^{B} P_{\mathrm{B},b} = P_{\mathrm{B}} \tag{10.23}$$

where P_{B} is the power of the battery bank. We will use the same convention to collectively refer to the power from the other components so that (10.22) can be concisely written as:

$$P_{\mathrm{gen}} + P_{\mathrm{B}} - P_{\mathrm{L}} - P_{\mathrm{DL}} - P_{\mathrm{BL}} = 0. \tag{10.24}$$

We use the term "total load" to refer to the sum of the power to the load, the diversion load and the ballast load.

10.6.1   Power Balance at DC and AC Buses

If we let $\sum P_{\mathrm{DC}}$ and $\sum P_{\mathrm{AC}}$ be the summation of the power associated with the components connected to the DC and AC buses, respectively, then the power balance for the whole system is

$$\sum P_{\mathrm{DC}} + \sum P_{\mathrm{AC}} = 0. \tag{10.25}$$

As suggested by (10.25), the sum of the power at each bus separately does not necessarily equal zero. An imbalance of generation, total load, and battery power at an individual bus is possible. When this occurs, power necessarily flows from one bus to the other through a rectifier, inverter, or bi-directional converter that links the buses. For simplicity, we will assume that a bi-directional converter links the buses. We use the convention that the power through the converter P_{con} is positive when the power flows from the DC bus to the AC bus. If the converter is a rectifier, then $P_{\mathrm{con}} \leq 0$; and if it is an inverter then, $P_{\mathrm{con}} \geq 0$.

The power through the converter is equal to the imbalance on the DC bus

$$P_{\mathrm{con}} = \sum P_{\mathrm{DC}} = P_{\mathrm{DC,gen}} + P_{\mathrm{B}} - P_{\mathrm{DC,L}} - P_{\mathrm{DL}} \tag{10.26}$$

which must be equal to the imbalance on the AC bus

$$P_{\mathrm{con}} = -\sum P_{\mathrm{AC}} = -P_{\mathrm{AC,gen}} + P_{\mathrm{AC,L}} + P_{\mathrm{BL}} \tag{10.27}$$

where the subscripts DC and AC are used to denote which bus the generation and load are connected to. Recall that batteries and diversion loads can only be coupled to the DC bus and the ballast load can only be coupled to the AC bus.
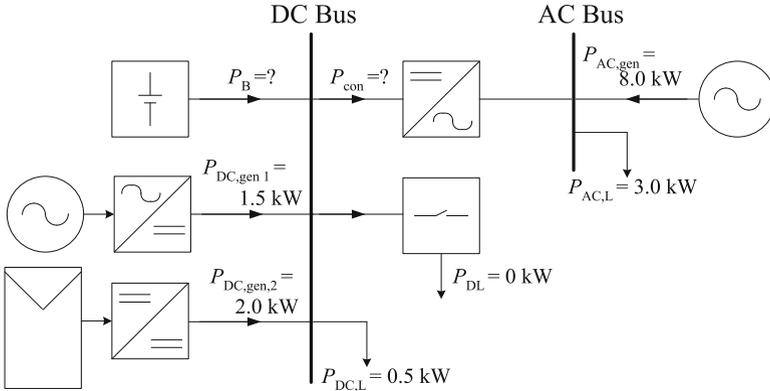
Fig. 10.15 Mini-grid for Example 10.5

Example 10.5 Consider the AC–DC-coupled mini-grid in Fig. 10.15. Compute the battery power and converter power.

Solution The battery power is computed by solving (10.24) for P_B

$$P_B = -\sum_{g=1}^{G} P_{gen,g} + P_L + P_{DL}$$

$$P_B = -1.5 - 2 - 8 + 3 + 0.5 + 0 = -8 \text{ kW}$$

The battery is therefore being charged. The converter power can be computed using (10.26) or (10.27). The AC bus has fewer components, so we use (10.27) to see $P_{con} = -8 + 3 = -5$ kW (rectifier mode).

10.6.2   *Including Losses*

The losses in a mini-grid occur within the components themselves and in the wiring between the components. In a well-designed system, the losses in wiring and connections are minimal, perhaps a few percent. The assumption hereafter is that all losses are included in the load. For example, a load of 100 W becomes 102 W when 2% losses are assumed. Generator losses are already included in P_{gen}, so their

power does not need to be adjusted. When losses are included, (10.26) and (10.27) are replaced with either (10.28) or (10.29), depending on the direction of power flow through the inverter:

$$P_{\text{con}} = \eta_{\text{con}} \sum P_{\text{DC}} = -\sum P_{\text{AC}} : \quad \sum P_{\text{AC}} < 0, \sum P_{\text{DC}} > 0 \quad (10.28)$$

$$P_{\text{con}} = -\eta_{\text{con}} \sum P_{\text{AC}} = \sum P_{\text{DC}} : \quad \sum P_{\text{AC}} \geq 0, \sum P_{\text{DC}} \leq 0 \quad (10.29)$$

Be mindful that η_{con} varies with power and direction of the power flow as discussed in Chap. 9.

Example 10.6 Repeat the previous example, but assume the inverter efficiency is 90%.

Solution We begin by computing the inverter power. We know $\sum P_{\text{AC}} = 8.0 - 3.0 = 5.0$ kW. This is positive, and so we use (10.29)

$$P_{\text{con}} = -\eta_{\text{con}} \sum P_{\text{AC}} = -0.90 \times (8 - 3) = -4.5 \text{ kW}.$$

so that 4.5 kW are supplied to the DC bus through the converter. Next, we apply (10.29) and again solve for the power to the battery bank:

$$P_{\text{con}} = \sum P_{\text{DC}} = P_{\text{DC,gen}} + P_{\text{B}} - P_{\text{DC,L}} - P_{\text{DL}}$$

$$-4.5 = (2.0 + 1.5) + P_{\text{B}} - 0.5 - 0$$

$$P_{\text{B}} = -4.5 - 3.0 = -7.5 \text{ kW}.$$

The losses in the inverter reduce the power flowing from the AC bus to DC bus. Subsequently, less power is supplied to the battery when compared to the lossless case.

10.6.3   Including Constraints

In actual mini-grids, the power associated with any component cannot exceed the component's rating. More generally, there are minimum and maximum limits that must be enforced in the power flow model, as discussed next.

10.6.3.1   Load Constraints

Under steady-state conditions, a load cannot consume more than its rated power, $P_{L,l}^{max}$, nor can it supply power. Therefore the following constraints are imposed:

$$0 \le P_{L,l} \le P_{L,l}^{max} \quad \forall l. \tag{10.30}$$

Some components such as motors temporarily consume power in excess of their rated value when starting up, in which case $P_{L,l}^{max}$ is variable.

Diversion and ballast loads cannot supply power or consume more than their rating:

$$0 \le P_{DL,m} \le P_{DL,m}^{max} \quad \forall m \tag{10.31}$$

$$0 \le P_{BL,n} \le P_{BL,n}^{max} \quad \forall n. \tag{10.32}$$

10.6.3.2   Generator Constraints

Generators are limited in the power they can provide:

$$P_{gen,g}^{min} \le P_{gen,g} \le P_{gen,g}^{max} \quad \forall g \tag{10.33}$$

where $P_{gen,g}^{max}$ and $P_{gen,g}^{min}$ are the maximum and minimum power that the generator can output. These limits might vary over time. There are three ways that the maximum power can be limited. The first is the generator cannot output more power than its rated value in steady state. The second is that the generator cannot output more power than input to it by the energy conversion device, minus the generator losses. This constraint often applies to PV arrays and WECS. The third is that the power can be limited by a controller. The constraint $P_{gen,g}^{max}$ is the lowest of these three limits. The minimum power cannot be negative, but it might be limited to a positive value. For example, a MHP system without a governor is unable to decrease the power it produces in steady state.

10.6.3.3   Battery Limits

The power into and out of a battery is limited by its SoC. A battery that is fully discharged cannot supply power; a battery that is fully charged cannot absorb power. More generally, the constraints on the battery power at any moment are:

$$P_B \le P_B^{max} \quad \text{(discharge limit)} \tag{10.34}$$

$$P_B \ge P_B^{min} \quad \text{(charge limit)}. \tag{10.35}$$

Note that per convention, P_B^{min} will be less than or equal to zero. The values of P_B^{max} and P_B^{min} battery depend on the SoC of the battery. The charging limit is enforced by the charge controller. It decreases in magnitude as the SoC increases, for example, as the controller transitions from the bulk to absorption stage. The discharge limit is enforced by the LVD of the charge controller, inverter or load. In the case where a LVD is not used, then the lower limit is dictated by the energy remaining in the battery.

10.6.3.4   Converter Limits

The power that can flow through a converter is limited to its rated power. This is expressed as the following constraints:

$$P_{con} \leq P_{con}^{max} \quad \text{(inverter mode : DC to AC)} \tag{10.36}$$

$$P_{con} \geq P_{con}^{min} \quad \text{(rectifier mode : AC to DC)} \tag{10.37}$$

If a converter is not bi-directional, then either P_{con}^{min} or P_{con}^{max} is set to zero.

10.7   Operation Priority Schemes

In mini-grids with multiple controllable components, there are often several ways that the power balance (10.22) can be maintained. For example, a decrease in load can be balanced by increasing the power to the diversion load or decreasing the gen set power output. While both actions are viable, the latter is preferred because it reduces fuel costs. The actions that a mini-grid can take in response to increases or decreases in load or uncontrollable generation should be prioritized by the designer and implemented in the mini-grid's control scheme.

A mini-grid should be operated in a way that minimizes fuel costs while achieving the desired reliability and availability targets. To do this, certain actions are given higher priority than others. An example of an operation priority scheme for an increase in load, or decrease in uncontrollable generation, is shown in Table 10.2. Uncontrollable generation refers to those whose power output cannot be changed on demand. The actions proceed in order, from one to the next, as applicable. The last and therefore least desirable action is shedding load, meaning part or all of the load is disconnected.

A priority scheme for a decrease in load (or an increase in uncontrollable generation) is shown in Table 10.3. It is similar to Table 10.2 but in reverse order. There are other considerations that might affect this scheme. For example, if the battery bank is at a low SoC, then charging it (priority 2) might be more desirable than saving fuel by decreasing power from the gen sets (priority 1). Priority 3, intentionally reducing the power from a source with no fuel cost—solar, wind, and hydro—is known as "throttling." Rather than throttling, it is usually better to

Table 10.2 Operational priority for increasing load (decreasing uncontrollable generation)

Priority	Action
1	Reduce power to the diversion load and ballast load
2	Increase power from zero-energy-cost resources (WECS, MHP, PV)
3	Increase power from the battery (discharge)
4	Increase power from fossil-fuel or biomass gen sets, starting with the least expensive
5	Reduce user load, starting with least critical

Table 10.3 Operation priority for decreasing load (increasing uncontrollable generation)

Priority	Action
1	Decrease power from fossil-fuel or biomass gen sets, starting with the most expensive
2	Increase power to battery bank (charge)
3	Decrease power from zero-energy-cost resources (throttle)
4	Increase power from diversion load or ballast load

increase the user load if possible so that some benefit is derived from the irradiance, wind speed, or water flow. For example, heating water and reducing the temperature in a freezer add meaningful load to the mini-grid. Discounted electricity rates might be offered to encourage use.

Priority schemes are implemented by the controllers in a mini-grid. As previously discussed, charge and diversion load controller set-points can be programmed so that, for example, the power from a PV array is reduced before the diversion load draws power. Controlling gen sets to follow the priority scheme is more complicated and often requires specialized controllers and the ability for the gen sets to automatically start-up and shut down. These aspects are discussed in the following sections.

There are other factors that affect the priorities in an operation scheme. For example, if the only source capable of forming the AC bus is the gen set, then the gen set must be continuously operated. Switching, for example, by LVD, can change the topology of the mini-grid. This can restrict the ability of AC-coupled sources to serve DC loads and DC-coupled sources to serve AC loads. Gen sets might also be operated to maximize their efficiency and to reduce their run times—which prolongs their lifespan—as discussed next.

10.8   Gen Set Control Schemes

The operation of gen sets described in Tables 10.2 and 10.3 is known as the "load-following" scheme. The gen set only produces as much power as is needed at any given time. It can be thought of as the default scheme. The gen set is only used when the power from the battery and renewable resources is insufficient to supply the load. This is basically how a hybrid electric vehicle operates.

Fig. 10.16 Schematic of the
PV system with DC load
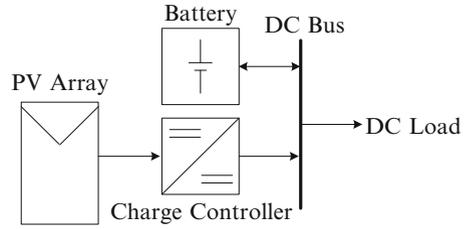
Alternatively, the gen set can be controlled according to a "cycle charging" scheme. In this approach, when the gen set is running it is loaded as high as possible, serving the load and charging the battery. The gen set shuts off when the battery reaches a predefined SoC as estimated by its terminal voltage. There are two benefits to this. The first is that the efficiency of gen sets increases with load (see Sect. 5.3.4); second, it limits the number of hours each day the gen set operates, prolonging its lifespan and reducing its noise pollution.

Automated cycle charging requires a sophisticated control system including a bi-directional converter (or a separate rectifier and inverter) with synchronization capability, a gen set with an auto-start feature, and a controller that coordinates the operation of the converter and gen set. There are commercially available products that can be used. Cycle charging can also be approximated manually. The operator switches from the inverter to the gen set when the load is expected to exceed the inverter rating (during the peak hours) and uses a battery charger to recharge the battery.

10.9   Examples of Mini-Grid Operation

To highlight how constraints, operation priorities and gen set control schemes affect the power flow in a mini-grid, we consider the three following illustrative cases. The cases are idealized in that they are based on simulation and that losses are ignored.

10.9.1   PV System with Battery-Constrained

We begin with a simple DC-coupled mini-grid consisting of a PV array, charge controller, battery, and DC load, as shown in Fig. 10.16. A simple system like this could be found in a stand-alone system providing LED lighting to a home. The power and SoC plots are shown in Fig. 10.17. The load is low overnight and during most of the day but has a sharp peak in the early evening, as is typical in most households. The power from the PV array follows the typical pattern of production under clear sky conditions.

Fig. 10.17 (**a**) Flow of power in an off-grid PV system. (**b**) The corresponding battery state-of-charge
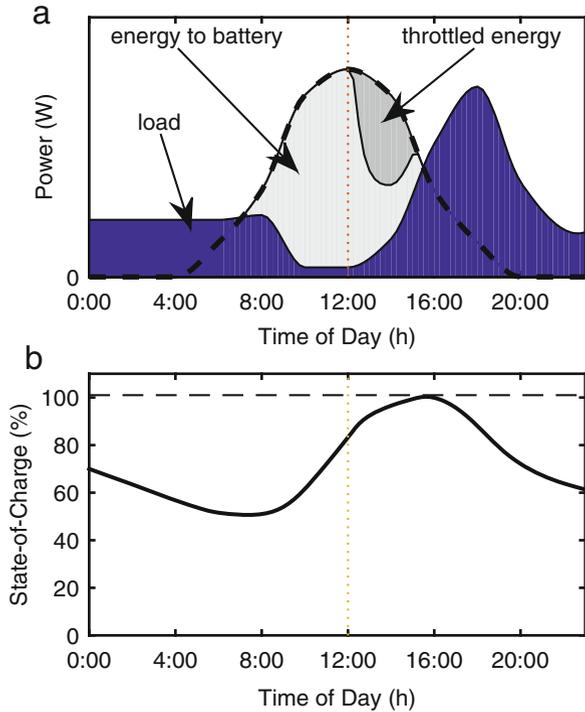
The vertical line at 12:00 shows when the absorption stage begins as the battery approaches a full SoC. The charge controller begins to throttle the PV array. Although this can be viewed as "wasted" power, in fact with the battery approaching a full SoC, it is an example of the power balance equation at work. There is simply nowhere for the power to go and so it is not produced. The power actually produced by the PV array and the power it is capable of producing diverge. The throttled energy is shown as the dark gray area in Fig. 10.17. This is the energy the PV array was capable of producing but did not. Throttling energy from PV arrays is a common side effect of the three-stage battery charging process.

10.9.2   Hybrid System—Load-Following

We next consider a hybrid AC–DC-coupled mini-grid consisting of a gen set, PV array, charge controller, battery, inverter with LVD and an AC-coupled load as shown in Fig. 10.18. The gen set is controlled using a load-following scheme and the priority list of actions are shown in Tables 10.2 and 10.3.

The mini-grid serves a somewhat unusual load that peaks in the morning as shown in Fig. 10.19a. The dashed white line is the gen set power output, and the gray
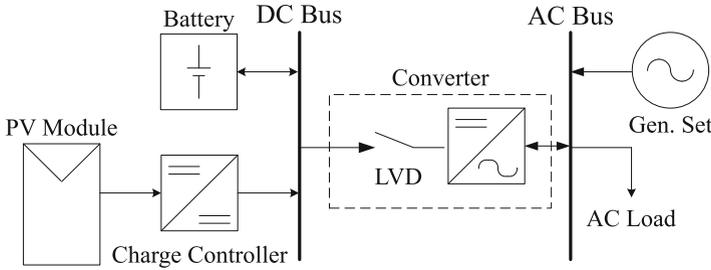
Fig. 10.18 Schematic of mini-grid used in load-following and cycle-charging examples

area is the energy produced by the PV array. The middle plot is the power through the bi-direction inverter. The bottom plot is the battery SoC. The SoC corresponding to the voltage that the LVD actuates is shown as $E_{\min}$.

We begin by conceptually assuming that just prior to time 0:00 (midnight), there is no load or generation. At 0:00, the load increases to the value shown in Fig. 10.19a. From Table 10.2, the first priority in balancing this increase in load is to reduce power to the diversion and ballast loads. This mini-grid has neither of these components, and so the second priority is considered: increase power from zero-fuel-cost sources (the PV array). This cannot be done when there is no sunlight, and so the third priority action is considered: discharge the battery. For the first few hours, the battery is able to supply the load. However, around 2:00 the load exceeds the inverter's power rating, and so the fourth priority is considered: increase power from the gen set. For this to happen, the gen set would need to be capable of automatically starting and synchronizing to the AC bus, perhaps initiated by a control signal sent by the inverter.

The battery continues to supply the maximum power allowed by the converter because it is the higher priority (lower cost) than the gen set. However, around 6:00, its LVD operates when the battery SoC becomes too low. The DC bus and AC bus are now isolated from each other, and the gen set supplies the entire load. The power from the PV array has a higher priority than the gen set. After sunrise its power output should increase while the gen set power decreases. However, this architecture does not allow the PV array to supply power to the AC bus unless the LVD has reconnected the DC bus to the AC bus. Therefore, the PV array power goes toward recharging the battery. Clearly the architecture of the mini-grid affects how the priority lists are implemented. On this day, the battery SoC does not increase enough for its terminal voltage to initiate a reconnection by the LVD. However, the load is fully served by the gen set.

Fig. 10.19 (**a**) Power from the gen set, PV array, and to the load when the gen set is controlled using a load-following scheme. (**b**) Power through the converter (positive is from DC bus to AC bus). (**c**) Battery state-of-charge
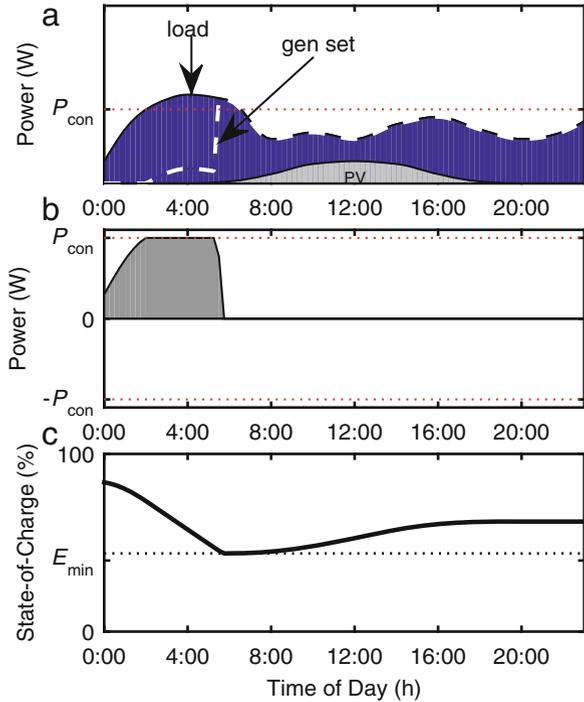
10.9.3   Hybrid System—Cycle Charging

We next consider the same mini-grid architecture as the previous case but with the gen set controlled using cycle-charging scheme and the converter being bi-directional. The operation is plotted in Fig. 10.20.

   At the start of the day (0:00), the load is served by the battery through the converter acting in inverter mode. At 2:00, the load has surpassed the converter's rating, as seen in Fig. 10.20b. The gen set begins producing power so that the load can be served. Because it is following a cycle-charging scheme, the gen set will produce as much power as possible, thereby operating at a higher efficiency. The gen set's power output is traced by the dashed line in Fig. 10.20a. The shaded area between the dashed line and the load is the energy used to recharge the battery. Note that the gen set produces rated power for several hours before tapering as the battery enters the absorption stage. At around 7:00, the battery is fully charged, and the load can be entirely supplied by the converter. The gen set therefore shuts down. Whenever practical, the PV array also begins producing power around this time. The PV array has the highest priority because it has zero fuel costs. However, it is not able to supply the entire load. From Table 10.2, the battery rather than the gen set is used to supplement the PV production.

Fig. 10.20 (**a**) Power from
the gen set, PV array and to
the load when the gen set is
controlled using a
cycle-charging scheme. (**b**)
Power through the converter
(positive is from DC bus to
AC bus). (**c**) Battery
state-of-charge
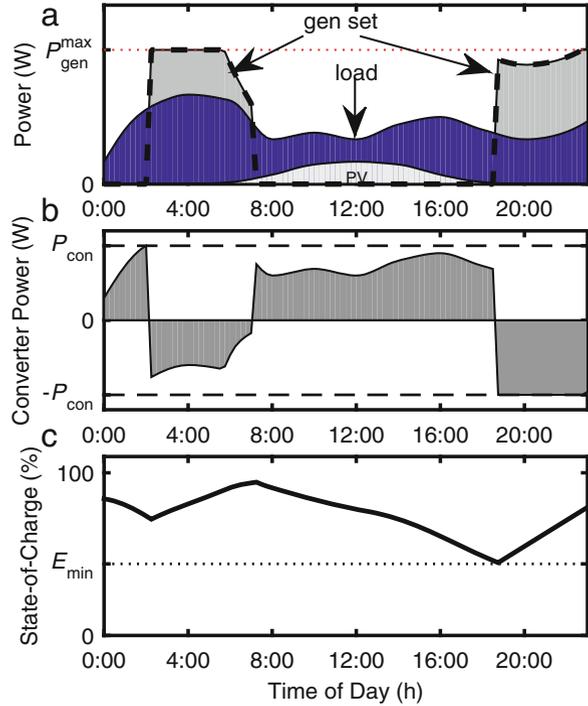
Around 19:00, the battery reaches its minimum SoC and cannot continue
supplying power. The gen set restarts and supplies the load while recharging the
battery. It is unable to produce its rated power due to the converter's power limit
(now acting as a rectifier).

Comparing Figs. 10.19 and 10.20, it is clear that the gen set's control scheme
greatly affects the operation of a mini-grid. Both load-following and cycle-charging
schemes are able to accomplish the basic function of supplying the load. However,
cycle-charging has the advantage of reducing the number of hours the gen set is
operated and it is operated at a more efficient loading point.

10.10   Parallel Generator Operation

We next consider the operation of an AC-coupled system with multiple synchronous
generators. This is a common architecture in mini-grids whose capacities exceed
100 kW and are powered by gen sets. A mini-grid of this size could likely serve
several hundred if not thousands households. Simultaneous operation of gen sets
connected to the same bus is known as "paralleling." Paralleling can also be done
with inverters and in general any group of AC generators, but we shall only consider

the case of gen sets. The same basic concepts broadly apply. A paralleled AC-coupled architecture offers the following benefits:

- Reliability—paralleling adds redundancy to the system so that if one gen set fails, a portion of or even the entire load can be served;
- Scalability—gen sets can be added or removed from the mini-grid as needed;
- Serviceability—maintenance can be done on one gen set at a time while the other(s) continue to serve the load.

Paralleled architectures are more complex to control and install, and are more expensive. Additional space is also required, but this is usually not a constraint in mini-grids in developing countries.

For gen sets to be operated in parallel, the generators must:

1. have the same number of phases;
2. have the same phase rotation (e.g., a-phase leads b-phase by 120°which leads c-phase by 120°);
3. have the same open-circuit terminal voltage at a given speed;
4. each have voltage and speed control, for example, through an AVR and a governor.

The voltage output by generators will not be perfectly sinusoidal. One factor affecting the distortion is the generator's "pitch factor." The pitch factor has to do with how the windings are physically arranged in the stator. We want the voltage waveform output by paralleled generators to as similar as possible, and so generators with the same pitch factor should be used—although this is not strictly required. The complexity of paralleling generators is greatly simplified if the gen sets are of the same model by the same manufacturer.

When paralleling generators, we are concerned with how they are synchronized, switched, and share load. Extra precaution is needed to protect the generators, for example, if the synchronism is done improperly or the control malfunctions. This can lead to conditions such as motoring, in which a generator operates as a motor, consuming real power.

10.10.1   Synchronizing and Switching

Generators should not be connected together until they are synchronized. Generators are synchronized when their terminal voltages have the same—or very nearly the same—frequency, phase, and magnitude. This can be done by an operator, with care, provided the speed and excitation of the generators can be manually adjusted.

Some gen sets can be synchronized through an external controller, as shown in Fig. 10.21. The control of the governor and AVR of each gen set is connected to this controller. It adjusts the excitation and speed until synchronization is achieved. After the generators are synchronized, they can be connected together. Manual or automatic transfer switches can be used to connect generators to the AC bus.

Fig. 10.21 Parallel operation of two gen sets using an external controller
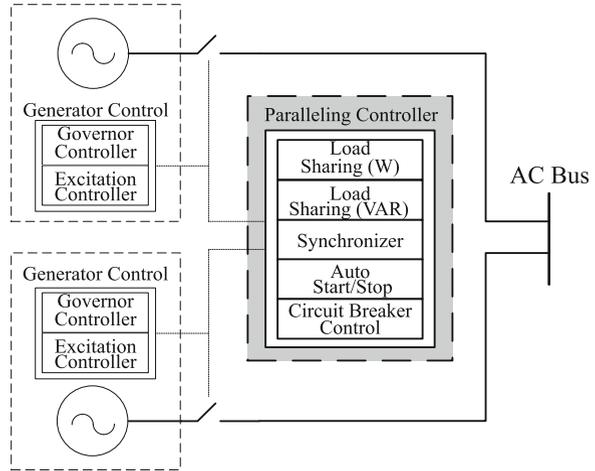
10.10.2   Load-Sharing

From the conservation of power, the sum of the real power from G-paralleled gen sets must equal the total load P_L (inclusive of losses). It can be shown that this must also hold true for the reactive power:

$$P_L = P_{\text{gen},1} + \cdots + P_{\text{gen},g} + \cdots + P_{\text{gen},G} \tag{10.38}$$

$$Q_L = Q_{\text{gen},1} + \cdots + Q_{\text{gen},g} + \cdots + Q_{\text{gen},G} \tag{10.39}$$

Load-sharing refers to how each gen set contributes to the real and reactive power required by the load [3]. In some situations each gen set contributes evenly, in which case

$$P_{\text{gen},1} = \cdots = P_{\text{gen},G} = \frac{P_L}{G} \tag{10.40}$$

and a similar expression holds true for reactive power. In some situations, equal sharing of the load is not desirable. In particular, one gen set might be larger or more fuel efficient than the rest. A common practice is to share the load in proportion to the gen sets' size. A larger-capacity gen set provides a larger share so that

$$P_{\text{gen},g} = P_L \times \frac{P_{\text{rated},g}}{\sum_{k=1}^{G} P_{\text{rated},k}} \tag{10.41}$$

where $P_{\text{rated},g}$ is the rated power of gen set g. Keep in mind that the efficiency of a gen set is very low at low loading. It is more fuel efficient when one generator operates at full capacity versus two at half. A good practice is to only turn on another gen set if the load is expected to exceed the capacity of those already supplying power. Regardless of how the load is to be shared, a control scheme is

Fig. 10.22 Droop curve for two gen sets; an isochronous curve is also shown
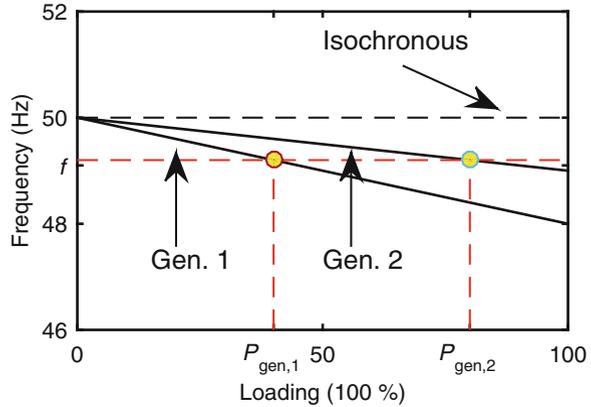
needed to implement the sharing. There are two general control approaches: droop and isochronous. The difference is how the gen set's governor responds to a change in load.

10.10.2.1 Droop Control

A simple approach to load-sharing is droop control. In this approach, each gen set is automatically and autonomously controlled by its governor so that as the power it supplies increases, its frequency *slightly* decreases (droops). For a gen set g, this is expressed as

$$f = f_{g,0} - d_g \frac{P_g}{P_{\text{rated},g}} \tag{10.42}$$

were f is the operating frequency when the gen set outputs real power P_g, and $f_{g,0}$ is the frequency of the gen set under no-load conditions—usually 50 or 60 Hz— and d_g is the droop slope [2]. When expressed graphically, (10.42) is known as the "droop curve." A droop curve is shown in Fig. 10.22 for two different gen sets each with a no-load frequency of 50 Hz but with different droop slopes.

We must keep in mind that the sum of the gen sets' power must equal that consumed by the load and that because the gen sets are in parallel, they operate at the same frequency. Under no load, the gen sets operate at their no-load frequency. In order for the gen sets to be paralleled, their no-load frequency must be the same. As the load increases, the frequency begins to decrease. See Sect. 5.2.5 for an explanation of why this happens. Each governor, sensing the reduction in frequency, responds by increasing the power produced by each gen set according to (10.42). The frequency will stabilize when the sum of the power from the generators matches the load. The system is at a new steady-state operating point, whose frequency is somewhat less than the no-load frequency.

Example 10.7 Consider a mini-grid with two gen sets operated in parallel. Gen set 1 is rated at 75 kW with droop slope of 0.6, and Gen set 2 is rated at 37.5 kW with a droop slope of 0.3. Both have a no-load frequency of 50 Hz. Determine the operating frequency and the power output by each gen set if the load increases to 60 kW.

Solution From (10.42), the droop for each gen set can be written as

$$f_1 = f_{1,0} - d_1 \frac{P_1}{P_{\text{rated},1}} = 50 - 0.6\frac{P_1}{75}$$

$$f_2 = f_{2,0} - d_2 \frac{P_2}{P_{\text{rated},2}} = 50 - 0.3\frac{P_2}{37.5}$$

According to the power balance, the sum of the generation must equal the load:

$$60 = P_1 + P_2.$$

Further, because the gen sets are operating in parallel, their frequencies must be the same in steady-state. Setting f_1 and f_2 equal to each other yields:

$$50 - 0.6\frac{P_1}{75} = 50 - 0.3\frac{P_2}{37.5}$$

$$P_1 = \frac{75}{0.6} \times 0.3\frac{P_2}{37.5}$$

$$P_1 = P_2.$$

Applying the power balance equation shows that each gen set produces 30 kW. The operating frequency is therefore:

$$f_1 = f_2 = 50 - 0.6\frac{30}{75} = 49.76 \text{ Hz}$$

In this case, the droops of the gen sets have been set so that the load is evenly shared. By selecting different relative values of d_1 and d_2, the load can be shared differently. For example, if each gen set had the same droop slope, then the power is shared in proportion to the rated capacity of each gen set.

A gen set's droop is often expressed as a percentage, calculated as:

$$Droop = 100 \times \frac{f_0 - f_{\text{FL}}}{f_{\text{FL}}} \tag{10.43}$$

where f_{FL} is the full-load frequency—the frequency when the generator is producing its rated power—and f_0 is the no-load frequency.

The gen sets share reactive power by adjusting their excitation. Recall from Sect. 9.11 that reactive power is sensitive to voltage magnitude. Therefore a voltage-based droop scheme can be used:

$$|V| = V_{g,0} - d_{\text{Q},g} \frac{Q_g}{Q_{\text{rated},g}} \tag{10.44}$$

where $|V|$ is the magnitude of the AC bus voltage, $V_{g,0}$ is the gen set's no-load (open-circuit) voltage, $d_{\text{Q},g}$ is the reactive power droop slope, and Q_g is the reactive power output of gen set g with rated reactive power $Q_{\text{rated},g}$.

An advantage of using droop control is that the generator's governors do not need to communicate with one another. They operate entirely autonomously. In fact, some gen sets will use droop control regardless of whether or not it is paralleled. The disadvantage of droop control is that the frequency and voltage magnitude varies somewhat with load.

10.10.2.2 Isochronous Control

Isochronous control is used in most newer or higher-end gen sets. The governor is automatically controlled so that the frequency is constant. The droop curve appears as a horizontal line, as in Fig. 10.22. Isochronous control of paralleled generators requires a separate controller to coordinate the load-sharing, as shown in Fig. 10.21. Should the communication fail, the generators default to droop-based control. If the generators tried to achieve isochronous operation without communicating to each other, the uncoordinated interaction of the separate controllers in each generator would likely cause the frequency and voltage to be unstable.

10.11 Maximum Power Point Tracking Algorithms

As detailed in Sect. 9.4, a maximum power point tracker (MPPT) is a DC–DC converter that is controlled so that a PV array operates at its maximum power point (MPP). This is an idealization. In practice, the MPP is constantly changing as irradiance and temperature change from one moment to the next. The MPPT then must constantly search for the MPP. There are several approaches for doing this [1, 4]:

- open-circuit voltage method
- short-circuit current method
- perturb and observe method
- incremental conductance method

Some of these approaches are simple and can be realized with an analog circuit. Others require a digital controller and sensors. The more sophisticated approaches are usually more expensive to implement as they require voltage and current sensors. In general they offer improved MPP tracking.

10.11.1 Open-Circuit Voltage Method

In this method, the open-circuit voltage of the PV array is periodically measured by the MPPT. The maximum power point voltage is assumed to be related to the open-circuit voltage V_{OC} by some constant k_v. The PV array voltage V_{PV} is controlled so that

$$V_{PV} = k_v V_{OC}. \qquad (10.45)$$

Typical values of k_v range from 0.73 to 0.80. To be effective, k_v is selected based on the parameters of the PV array the MPPT is connected to. The MPPT is therefore not "plug-and-play," as it must be custom-programmed for a given array. Since the relationship between the open-circuit and MPP voltage is not constant, the PV array does not necessarily operate at the true MPP. In addition, the PV array must be periodically open-circuited to measure the voltage, which somewhat reduces the average power output.

10.11.2 Short-Circuit Current Method

This method is similar to the open-circuit method, but the short-circuit current is measured instead of the open-circuit voltage. The PV array current I_{PV} is controlled such that

$$I_{PV} = k_i I_{SC}. \qquad (10.46)$$

Values of k_i typically range from 0.78 to 0.92, depending on the parameters of the PV array. Like the open-circuit method, the power output is periodically interrupted, and the array does not necessarily operate at the true MPP. It is generally more accurate and efficient than the open-circuit method. However, it requires a current sensor which generally is more expensive and less accurate then a voltage sensor.

Fig. 10.23 Example of the PO algorithm at various steps
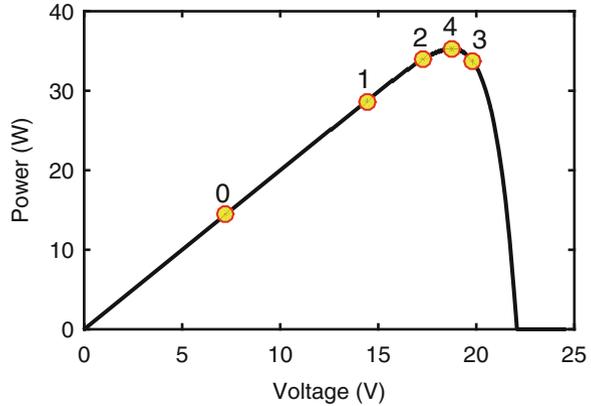
10.11.3   Advanced Methods

Most MPPTs use control algorithms to continuously adjust V_{PV} as environmental and load conditions change. The most common are the perturb and observe (PO) and the incremental conductance (IC) methods. These methods are widely used in commercially available MPPTs. Both methods require voltage and current measurements but are not dependent on the parameters of the PV array. We will discuss the PO method next. The reader can consult references such as [1, 4] for additional details on the IC and other methods

The PO method uses a "hill-climbing" approach. Hill-climbing approaches use an iterative method for finding the maximum power point voltage V_{PV}^*. Consider the $I-V$ and power characteristic shown in Fig. 10.23. Notice that the power curve resembles a hill, with the maximum power point at the top of the hill. Assume the present operating point of the PV module is at point (0). Although from the figure we can readily identify the location of the maximum power point, the MPPT must only rely on current and voltage sensors at its present or past positions to determine if the voltage should be increased or decreased to increase the power output. In other words, it cannot "see" the entire hill. Different algorithms employ a variety of methods to determine which voltage direction is "up-hill", how large of a step to take in that direction, and then adjust the duty cycle to the DC–DC converter accordingly. The result is a sequence of operating points that lead to the top of the hill as shown by the numbered operating points (0)–(4) in Fig. 10.23. It is unlikely that the algorithm will arrive at the top of the power curve without overshooting, shown as point (3), in which case the algorithm identifies that decreasing the voltage will increase the power, eventually leading to point (4), the maximum power point.

The PO method is based on the idea that the sign of the derivative of the power with respect to voltage can be used to tell if the voltage should be increased or decreased to reach the MPP:

$$\frac{\mathrm{d}P}{\mathrm{d}V} < 0 \quad \text{MPP is left of present position (voltage too high)} \qquad (10.47)$$

$$\frac{\mathrm{d}P}{\mathrm{d}V} = 0 \quad \text{MPP has been reached} \qquad (10.48)$$

$$\frac{\mathrm{d}P}{\mathrm{d}V} > 0 \quad \text{MPP is right of present position (voltage too low).} \qquad (10.49)$$

In practical applications, the derivative is approximated as a difference. Let the voltage and power at time t be $V[t]$ and $P[t]$, respectively. The voltage is directly measured; the power is computed as the product of the measured voltage and current. The derivative is approximated as:

$$\frac{\mathrm{d}P}{\mathrm{d}V} \approx \frac{\Delta P}{\Delta V} = \frac{P[t] - P[t-1]}{V[t] - V[t-1]} \qquad (10.50)$$

If the result is negative, then the voltage $V[t]$ is too low. At the next time step, the voltage is perturbed in the positive direction by some step size α:

$$V[t+1] = \alpha + V[t]. \qquad (10.51)$$

The step size can be fixed, for example, 0.1 V, or it can be based on the magnitude of (10.50). The voltage change from one step to the next is achieved by adjusting the duty ratio of the DC–DC converter.

Despite the conceptual simplicity, PO methods tend to oscillate around the MPP, resulting in submaximal power output. PO methods have slower convergence than some other methods, in particular when irradiance rapidly changes. For example, the PO method does not know if an increase in power after a perturbation is because the MPP is being approached or if the irradiance increased. This can lead the PO to perturb in the incorrect direction. The operating point can also be "trapped" at a local maximum in the power-voltage curve that occurs when part of the PV array is shaded. PO methods can be implemented using analog circuits or a simple digital controller.

Example 10.8 In this example, the perturb and observe method with variable step size is demonstrated. The I–V curve of a PV module in Fig. 10.24 is considered. The important values for each of the first several steps are provided in Table 10.4. The starting point (step 0) is arbitrarily selected as 12 V with a positive initial perturbation of 0.1 V in the positive direction. For simplicity, we assume that the I–V curve does not change. The step-size magnitude is set to

$$|\alpha| = \frac{1.5}{I[k]} \times \left| \frac{\Delta P[k]}{\Delta V[k]} \right|$$

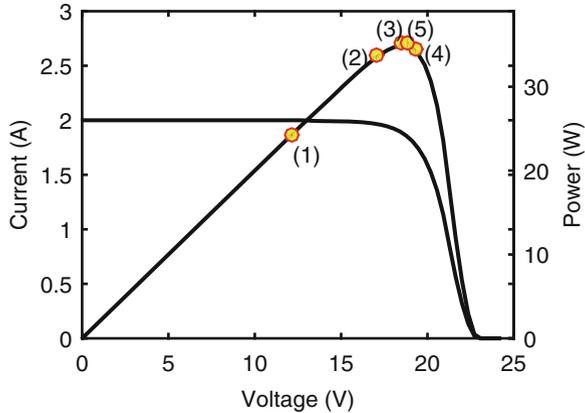**Fig. 10.24** The $I-V$ and power characteristics for the module in Example 10.8


Table 10.4 Example of perturb and observe method

Step	V	I	P	ΔP	ΔV	α
0	12.00	2.00	24.00	–	–	0.10
1	12.10	2.00	24.20	24.20	0.10	5.00
2	17.10	1.97	33.64	9.44	5.00	1.44
3	18.54	1.89	35.11	1.47	1.44	0.81
4	19.35	1.79	34.61	−0.51	0.81	−0.53
5	18.82	1.87	35.11	0.50	−0.53	0.77

with a maximum value of 5.0. The reader should confirm the values in the table. The actual MPP is 35.13 W. Note that the algorithm nearly obtains this value in step 3 and then overshoots it, before returning.

10.12 Summary

This chapter covered how off-grid systems, mini-grids in particular, are controlled to achieve the desired balance of power among and between its components. Off-grid systems are generally controlled to minimize operating costs, maximize reliability, and prolong the life of their components. The charging and discharging of batteries require special consideration as their lifespan and performance can be threatened if the system is not properly operated. Most batteries are charged using a three-stage approach consisting of bulk, absorption, and float stages. The terminal voltage and battery current associated with each stage have a distinct profile. Inspection of the voltage profile in particular is useful in qualitatively assessing the health of the system and understanding if it is functioning properly.

Fig. 10.25 Mini-grid for
Problem 3 and 4
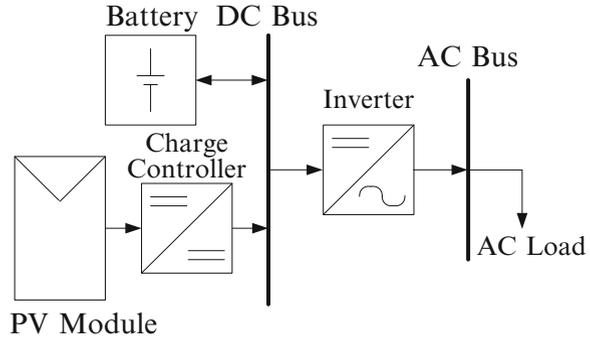
A steady-state algebraic power flow model was developed for a system with multiple sources. The model is based on conservation of power. The model can be combined with the operation scheme of the mini-grid to analyze and simulate it. Operation schemes show the priority of actions that should be taken as load and generation from uncontrolled sources change. They are usually based on minimizing the operational cost of the mini-grid. When multiple generators or inverters are coupled to the AC bus, they must be synchronized. Droop or isochronous control can be used to share the real and reactive power between the generators. The chapter also covered different maximum power point tracking methods for PV arrays.

As we proceed in the next chapters to discuss the design of off-grid systems, we should not forget that the operation and control of the mini-grid require careful consideration prior to implementation.

Problems

10.1 Describe, in your own words, the purpose of each stage in a three-stage battery charging process.

10.2 Sketch a charging plot (voltage) of a 24 V system with the following set-points: $V_{abs} = 28.4$ V and $V_{float} = 27$ V. Assume the battery's initial voltage is 26 V, and the absorption stage lasts for 4 h.

10.3 Consider the mini-grid in Fig. 10.25. The AC load current is 17.5 A. The battery resistance is 0.09 Ω. The battery is being charged in the absorption stage with set-point 14.2 V. The state-of-charge voltage V_{SoC} is 12.1 V. What is the current from the charge controller? What is the required power from the PV array assuming the charge controller's efficiency is 95%?

10.4 Consider the mini-grid in Fig. 10.25. The AC load current is 9.1 A. The battery resistance is 0.09 Ω. The battery is being charged in the absorption stage with set-point 14.2 V. The state-of-charge voltage V_{SoC} is 12.1 V. The charge controller is

Fig. 10.26 Mini-grid for
Problem 5, 6 and 7
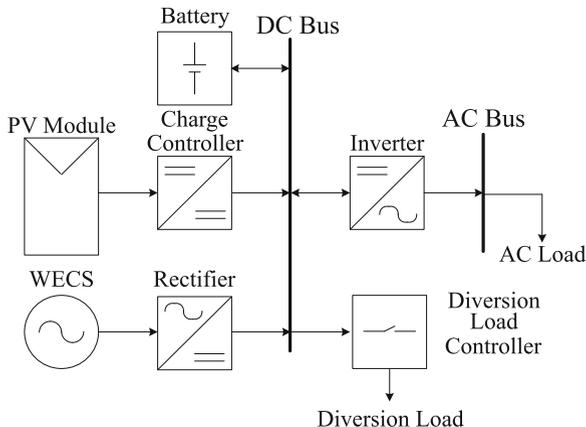
power-constrained due to a cloud reducing the irradiance. The maximum charge controller current is 11 A. Determine the battery's terminal voltage and comment on whether or not the terminal voltage is able to be regulated at the absorption stage set-point.

10.5 Consider the mini-grid in Fig. 10.26. The power from the PV array is 10 kW and the load is 16 kW. The battery is in the bulk charging stage, and so the diversion load is not consuming power. Compute the power required from the WECS to charge the battery with 2 kW if the inverter efficiency is 85%.

10.6 Consider the mini-grid in Fig. 10.26. The charge controller absorption set-point is 57.6 V; the diversion load set-point is 58.4 V. The battery is being charged in the absorption stage. The state-of-charge voltage V_{SoC} is 52 V. The current from the wind turbine is 56 A. The load current is 19 A. The battery resistance is 0.10 Ω. Compute the battery terminal voltage and current from the charge controller and to the diversion load, if any.

10.7 Consider the mini-grid in Fig. 10.26. The charge controller absorption set-point is 57.6 V; the diversion load set-point is 58.4 V. The battery is charged in the absorption stage. The state-of-charge voltage V_{SoC} is 52 V. The current from the WECS is 74 A. The load current is 8 A. The battery resistance is 0.10 Ω. Compute the battery terminal voltage and current from the charge controller and to the diversion load, if any.

10.8 Consider a mini-grid with two gen sets connected in parallel to the AC bus. Gen Set 1 is rated at 100 kW with droop slope of 0.15 and no-load frequency of 60 Hz. Gen Set 2 is rated at 80 kW with droop slope of 0.13 and no-load frequency of 60 Hz. Compute the power output and frequency of each gen set when the load is 110 kW.

10.9 Consider the gen sets in the previous example. The reactive power droop slope for Gen Set 1 is 10.0 and 8.0 for Gen Set 2. The no-load voltages are 230 V. The rated reactive power for Gen Set 1 is 65 kVAR and 50 kVAR for Gen Set 2. Compute the reactive power output and voltage magnitude of each gen set when the reactive power of the load be 60 kVAR.

10.10 What must the relationship between the droops, in percent, be for three gen sets rated at 50 kW, 75 kW, and 100 kW be for the power to be shared (1) equally among the gen sets or (2) in proportion to the rating of the gen sets?

10.11 Consider the plots in Fig. 10.27. Identify if the gen set is being operated in a load-following or cycle-charging scheme. Explain your reasoning.

10.12 Write a perturb and observe algorithm using a computer language to find the MPP of a PV module with the following parameters: $I_0 = 8 \times 10^{-10}$ A, illumination current of 4 A, and $V_T = 0.0258$ V. The module has 60 series-connected cells. Ignore the shunt and series resistance of the PV module.

Fig. 10.27 Mini-grid for Problem 11
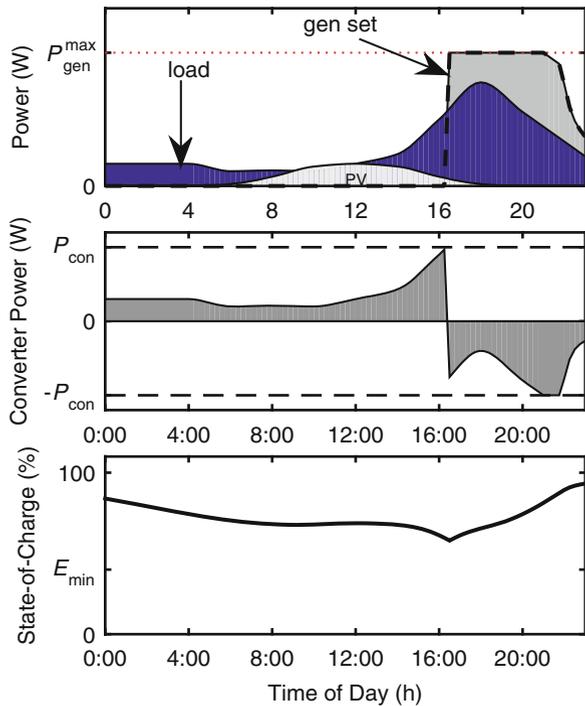
References

1. Joshi, P., Arora, S.: Maximum power point tracking methodologies for solar PV systems – A review. Renew. Sustain. Energy Rev. **70**, 1154–1177 (2017). doi:https://doi.org/10.1016/j.rser.2016.12.019. URL http://www.sciencedirect.com/science/article/pii/S1364032116310826
2. Lopes, J.A.P., Moreira, C.L., Madureira, A.G.: Defining control strategies for MicroGrids islanded operation. IEEE Trans. Power Syst. **21**(2), 916–924. https://doi.org/10.1109/TPWRS.2006.873018
3. Olson, G.: Paralleling dissimilar generators: Part 3 – load sharing compatibility. Tech. Rep. 9017, Cummins Power Generation (2010)
4. Ram, J., Rajasekar, N., Miyatake, M.: Design and overview of maximum power point tracking techniques in wind and solar photovoltaic systems: A review. Renew. Sustain. Energy Rev. **73**, 1138–1159 (2017). doi:https://doi.org/10.1016/j.rser.2017.02.009. URL http://www.sciencedirect.com/science/article/pii/S1364032117302137
5. Vader, R. (ed.): Energy Unlimited. Victron Energy (2011)
6. Zimmerman, R.D., Chiang, H.D.: Fast decoupled power flow for unbalanced radial distribution systems. IEEE Trans. Power Syst. **10**(4), 2045–2052 (1995). doi:10.1109/59.476074